Biosensors and Bioelectronics 202 (2022) 113996

Contents lists available at ScienceDirect

Biosensors and Bioelectronics

journal homepage: www.elsevier.com/locate/bios

Differential Impedance Sensing platform for high selectivity antibody detection down to few counts: A case study on Dengue Virus

Paola Piedimonte [a,*], Laura Sola [b], Marina Cretich [b], Alessandro Gori [b], Marcella Chiari [b], Edoardo Marchisio [d], Piero Borga [c], Riccardo Bertacco [c], Andrea Melloni [c], Giorgio Ferrari [a], Marco Sampietro [a]

[a] Department of Electronics Information and Bioengineering, Politecnico di Milano, Piazza L. da Vinci 32, Milan, 20133, Italy
[b] National Research Council, Istituto di Scienze e Tecnologie Chimiche (SCITEC-CNR), Via M. Bianco 9, Milan, 20131, Italy
[c] Department of Physics, Politecnico di Milano, Piazza L. da Vinci 32, Milan, 20133, Italy
[d] Dia.Pro - Diagnostic Bioprobes S.r.l., Via G. Carducci 27, Sesto San Giovanni MI, 20099, Italy

ARTICLE INFO

Keywords:
Impedance detection
Differential impedance sensing
DIS
Biosensor
Antibody detection
Diagnostic platform
Immunosensor

ABSTRACT

We developed a biosensing system for serological detection of viruses based on the impedance variation between gold microelectrodes upon the capture of the target antibodies hybridized with nanobeads for signal amplification. The microfluidic platform core features a Differential Impedance Sensing (DIS) architecture between a reference and an active sensor able to reach nanoparticle resolution of few tens. The biosensor, functionalized with a copoly layer housing a synthetic peptide probe, has shown a limit of detection (LOD) below 100 pg/mL using a model IgG antibody spiked in a buffer. The biosensor was also tested with human serum samples for quantitative counts of anti-Dengue Virus antibodies, reaching a sensitivity that outperforms commercial ELISA kit. The system is perfectly suited to be easily reconfigured for novel probes by simply modifying the preparation of the biosensor chip surface, thus addressing a wide range of pathogens and diseases with clinically relevant concentrations for rapid immunoassays in a point of care setting.

1. Introduction

In a world where the movement of people has reached its high for leisure, migratory and working reasons, new infections may arise and quickly spread throughout. Dengue, Chikungunya, Zika and respiratory viruses such as coronaviruses are unfortunately taking the stage of public concern (Bhatt et al., 2013; Guzman et al., 2010; Herrada et al., 2018; Merkoci et al., 2021; Messina et al., 2019). Consequentially, serological assays are being widely studied and used for infection screening as relatively cheap and easy to operate approaches compared to infected cell culture or nucleic acid based methods. In addition, to be relevant for early diagnosis, specific antibody detection is important for epidemiological surveillance and for the evaluation of the risk of severe pathologies, especially in the frame of vaccination campaigns. In this context, the availability of simple and inexpensive point-of-care platforms would spread the use of serological tests even in low-resource settings where the actual numbers of cases are still underreported (Ozer et al., 2020). The current gold standard for antibody detection relies on enzyme-linked immune-sorbent assay (ELISA) (Alcon et al., 2002; Lequin, 2005). However, this test is time and reagent-consuming and does not have multiplex capability, thus not allowing the detection of several targets at the same time (Desmet et al., 2013). Furthermore, the fluorescence based detection represents a limit in terms of digital count and single molecule detection (Cohen and Walt, 2019). Alternatively, a large number of biosensors concepts have been developed to measure the presence of analytes by combining the sensitivity of biomolecular recognition elements with a physical transduction mechanism like Surface plasmon resonance-based technologies (SPR) (Austin Suthanthiraraj and Sen, 2019; Singh, 2016; Wijaya et al., 2011), Electrochemical sensing (ES) (Chowdhury et al., 2019; Tancharoen et al., 2019) and Electrochemical Impedance Spectroscopy (EIS) (Lisdat and Schäfer, 2008; Ohno et al., 2013). Their advantages include a high sensitivity and specificity provided by the biocatalytic or biorecognition sensing elements resulting in time-effective, low-cost, and easy-to-use analytical tools. Some of them are particularly suitable for miniaturization and portability thanks to the increase of the electronic content in

* Corresponding author.
E-mail address: paola.piedimonte@polimi.it (P. Piedimonte).

https://doi.org/10.1016/j.bios.2022.113996
Received 2 November 2021; Received in revised form 3 January 2022; Accepted 10 January 2022
Available online 15 January 2022

their operation and to the detection of the signal based on the interaction of the biological recognition element with the analyte. These devices indeed depend on the evaluation of currents and/or voltages to detect binding (Nadzirah et al., 2015) or on the electrical property changes (complex impedance, resistance, or capacitance) of electrodes (Berggren et al., 2001; Qureshi et al., 2010).

Here we present a biosensor system that merges a sophisticated biochemistry recognition mechanism into an advanced miniaturized platform based on Differential Impedance Sensing (DIS). The system is based on measuring the impedance variation between interdigitated microelectrodes upon the capture of the target antibodies on the surface of an insulating borosilicate chip. Differently from Electrochemical biosensors as faradaic EIS (Orazem and Tribollet, 2008) that targets electron transfer at the electrode-electrolyte interface to provide information about the nature and rate of probe-target binding, here we amplify the impedance signal at a single frequency by hybridizing the probe-target compound with a functionalized polystyrene bead. Compared to faradaic EIS, DIS does not require measurements and data fitting over a wide range of frequencies nor the use of a potentially hazardous redox couple for measuring a charge transfer, thus easing the experimental protocol perspective. Mainly, DIS measures the impedance at a relatively high frequency to sense the perturbation provided by the insulating bead to the electrical properties of the liquid volume between the microelectrodes. On the contrary, standard EIS senses at a low and medium frequency the electrical properties of the electrode-liquid interface where the surface functionalization of the electrode is a critical step that should be carefully designed for each biosensor to obtain a stable and electrically effective interface (Bertok et al., 2019; Darwish et al., 2018; Garrote et al., 2019; Pellitero et al., 2020). The laborious preparation of the surface, the usually limited storage time of the sensor, and the biofouling of the surface occurring in no purified samples (Pinkova Gajdosova et al., 2021) are drawbacks that can be overcome by the increased signal-to-noise ratio offered by the bead signal amplification. Moreover, the single-frequency measurements and data analysis on the enhanced signal simplifies the platform hardware and software, enabling portable analysis.

The impedance measurement in DIS is performed as the impedance difference between an active sensor, functionalized with the biological probes, and a reference sensor, twin but without probes and placed near the active one. This setting ensures the measurement to be insensitive to temperature fluctuations and to variation of the liquid medium of the assay (i.e. salinity concentration) that would alter both sensors in the same way, thus allowing high stability of DIS results over time. The electrodes for DIS are not active/reactive as required in ES and therefore do not call for special elemental compositions as Ag/AgCl or carbon used in recent reports (Liang et al., 2019; Strong et al., 2021) they should only be biocompatible and they require few standard technological steps ensuring competitive costs.

The paper describes in detail the design and fabrication of the chip, the biochemical functionalization of the surface, and the tests to address and quantify the performance of the entire platform. Finally, to highlight the effectiveness of the DIS approach in counting the number of beads, we tested the flexibility of the platform by detecting the Dengue virus (DENV) in human serum (Kabir et al., 2021; Martina et al., 2009; Zhang et al., 2015) and compared the results with those obtained by a standard laboratory procedure. To this aim, a synthetic peptide was designed and synthesized (Bergamaschi et al., 2019; Cretich et al., 2011) to mimic the antigenic determinant of Dengue full envelope protein forming the outermost layer of the virion particle. It has been chemoselectively grafted over the biosensor surface to target anti-Dengue Virus antibodies. The immunodiagnostic performance of the peptide in discriminating Dengue infected individuals from healthy controls is comparable with that of the full protein E with advantages in terms of preparation, manipulation, and cost (Gori et al., 2016). The proposed system paves the way for the development of a lab-on-a chip system for the rapid diagnosis of infectious diseases with very high sensitivity, down to single-molecule counting.

2. Materials and methods

2.1. Sensors design, fabrication and operation

The interdigitated gold microelectrodes have fingers of 3 μm width, 90 μm length and 3 μm spacing. The choice of the beads size (800 nm) has been a trade-off between 1) the importance of an optical microscope feedback for the visual proof of the beads selective binding over the active region and 2) the effective robustness in binding capability. Accordingly, we designed the electrodes using COMSOL simulations results to achieve the maximum impedance variation for one bead detection. The resulting area of the microelectrodes is 90×90 μm^2 to match the minimum spotting size of the machine used to functionalize the chip surface, lead to a dynamic range of about 1 part over 13000 given by the full coverage of the sensing area by a layer of beads. From Finite Element Method simulations (COMSOL Multiphysics) of the sensor implemented as described in (Carminati et al., 2014), a single bead residing on the IDE surface would give a signal of about 15 mΩ (from 14 mΩ if placed over the electrode to 16 mΩ if situated within the IDE gap), allowing for close correlation of beads numbers and DIS signals.

The sensors were fabricated on a 3-inch borosilicate wafer (Micro-Chemicals GmbH) using conventional microfabrication techniques and lithography process. First, the substrate has been cleaned with acetone, isopropyl alcohol, DI water sonication, and dried by N2 and 120 °C hotplate. The Ti primer and the image reversal AZ5214E photoresists have been deposited by spin coating at 6000 rpm for 60 s and soft baked at 110 °C for 90 s. The photolithography step was realized with Maskless Aligner - Heidelberg MLA100. The Cr/Au (5/120 nm) was deposited by Thermal Evaporator - Moorfield MINILAB-080 with a 0.5 A/s deposition rate. Chips are sonicated in acetone for full lift-off of photoresist, washed with double-distilled water and dried by a stream of nitrogen. A 5 μm SU8 layer was used to make micro-windows on the metal patterns over the sensing area and a passivation layer of the metal electrodes elsewhere.

Sensors have been designed in differential pairs (Fig. 1) to fully exploit bead signal amplification without the burden of the total impedance level: only one sensor of the pair is functionalized with the probe, the other not being functionalized or having a negative control. The system is tuned to a zero-output signal before starting the assay. The binding of a bead on a target molecule captured by the probe unbalances the differential pair and generates a net output signal. This technique grants to adjust the gain of the electronic instrumentation to limit the effect of slow fluctuations in the gain of the lock-in amplifier used for impedance measurement (Carminati et al., 2016; Gervasoni et al., 2017). Furthermore, the differential architecture is insensitive to the macroscopic fluctuations of the assay in terms of temperature and of liquid medium composition, leading to a very stable and easy-to-use set-up for effective point-of-care measurements.

2.2. Biochip preparation

The functionalization of the chip for probe immobilization was obtained by coating the entire chip with a copolymer, namely MCP6, able to form a stable nanometric film on different materials (glass, gold, silicon, thermoplastics …). Copolymer MCP-6 is obtained from the post-polymerization modification of the functional monomer of a common precursor, MCP2 (synthesized by free radical polymerization using 2,2′-Azodi (isobutyronitrile) (AIBN) as thermo-initiator), which is composed of N,N-dimethylacrylamide (97% molar fraction), N-acryloyloxysuccinimide (2% molar fraction), and 3-(trimethoxysilyl)- propyl methacrylate (MAPS, 1% molar fraction) (Sola et al., 2016) The amphiphilic behavior of N,N-dimethylacrylamide (DMA), which constitutes the polymer backbone, allows the formation of a stable and

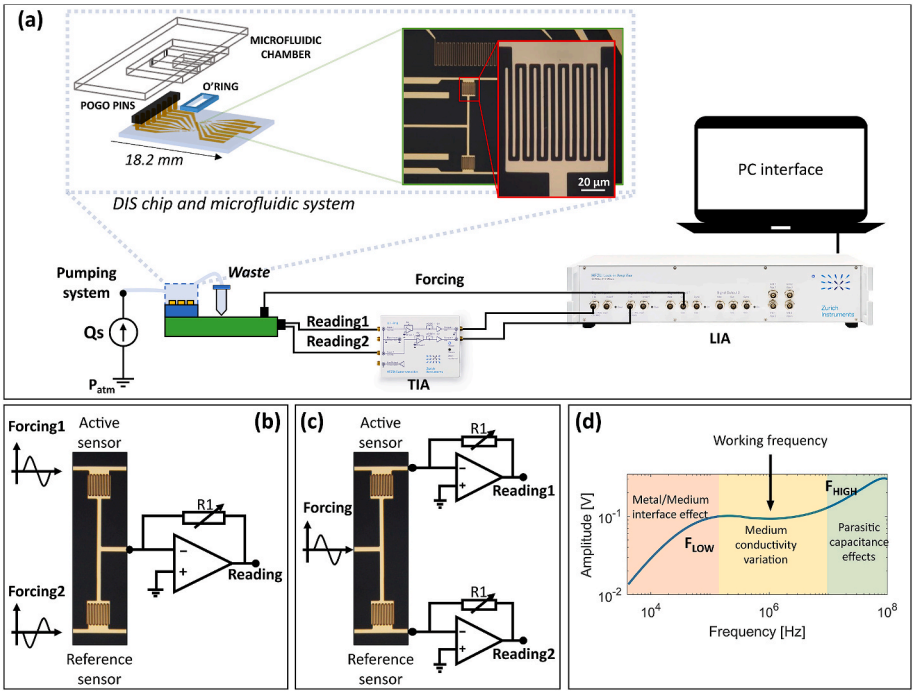

Fig. 1. (a) Photographs of the sensor and schematic view of the microfluidic system of the measuring set-up for the Differential Electronic Impedance. The two available configurations to perform Differential Impedance Sensing (DIS): analogic differential operation (b) and offline digital differential operation (c). (d) Full spectrum of impedance as a function of frequency in PBS solution, the chosen working frequency around 1 MHz will assure to work in the region medium conductivity variation.

hydrophilic nanometric film by a combination of hydrogen bonds, van der Waals and hydrophobic interactions. The silane monomer (MAPS) strengthens the bonding of the polymer to the surface through the formation of covalent bonds with hydroxyl or silanol groups. Finally, the third monomer NAS confers chemical reactivity to the copolymer. Recently the high reactivity of NAS towards nucleophiles (such as amine) was exploited to generate a family of polymers bearing functional groups that allow probe coupling through click chemistry reactions. In particular, MCP-6 obtained by modifying the parent polymer's functional monomer NAS with 3-azido-1-propylamine (Sola et al., 2016) bears azide functionalities which react via the Strain-promoted azide-alkyne cycloaddition (SPAAC) reaction with the DBCO group, synthetically introduced into the probe. The orthogonality offered by the click chemistry reactions favors the accurate control of the probe orientation on the surface, positively affecting the analytical outcome of the assays. Peptide E01, modified with DBCO group, has the following sequence: DBCO-(O2Oc)2-DRGWGNGCGLFG and has been synthesized as reported in (Gori et al., 2016). The polymer forms a functional film on the entire surface, but thanks to the use of a robotic dispensing system (spotter) it was possible to immobilize the peptide E01 in precise and specific locations thus avoiding non-specific binding of the target outside the electrode area, during the following step of the experiment. Moreover, this phenomenon is also prevented by the fact that azide groups do not react with functionalities naturally present in biomolecules. E01, used as a proof of concept, is a peptide able to mimic the antigenic performance of Dengue envelope protein (E), which forms the outermost layer of the virion particle. The density of the peptide immobilized on the surface was calculated using the Interferometric Reflectance Imaging Sensor (IRIS) platform. In this label-free technique, by the use of previously determined calibration factors, a quantification of the amount of probe mass that is bound at each spot location (Cretich et al., 2012).

Chips were pretreated using a HARRICK Plasma Cleaner, PDC-002 (Ithaca, NY, USA) connected to an oxygen line. Chips were functionalized immersing in 1% w/v solution of MCP-6 copolymer (Lucidant Polymers Inc., Sunnyvale CA, USA) containing 0.8 M ammonium sulfate. Peptide E01 (DRGWGNGCGLFG), modified with a terminal DBCO group, has been designed and synthesized as reported in (Cretich et al., 2011). It was diluted to 100 μM using a 15 mM sodium acetate buffer containing 25 mM trehalose. Concentration of the peptide E01 and spotting buffer composition was optimized to provides the most-uniform and reproducible binding in terms of spot shape and probe density, in the order of 1–1.8 ng/mm2 (Gori et al., 2016). Similarly, the concentration of secondary antibody and PS nanobeads have been chosen to assure a large excess of molecules with respect to those captured by the spotted peptide. In this way, they are not limiting reagents, maximizing the binding to the analyte and consequently the detectable signal. Rabbit anti-E01 IgG was a kind gift from Primm (Milano, Italy); the biotinylated goat anti-rabbit IgG for buffer measurements and the biotinylated rabbit anti-human IgG for human serum experiments have been purchased from Life Technologies, Thermo Fisher Scientific.

The spotting over the sensor area was performed using a Sci-FLEXARRAYER S12 (Scienion, Berlin, Germany) at 20° C in an atmosphere of 60% humidity. After spotting, the chips were stored overnight at room temperature in a sealed chamber, saturated with sodium chloride (40 g/100 mL H_2O). After overnight incubation, the chips were rinsed by immersing them into a 2 mM EDTA solution for 1 h at room temperature, then rinsed with DI water and dried with a nitrogen stream.

In the human serum experiments we used a washing buffer (0.05M Tris HCl pH 9, 0.25 M NaCl, 0.05% Tween 20) and an incubation buffer (0.05M Tris HCl pH 7.6, 0.15 M NaCl, 0.02% Tween 20). Other chemicals were from Sigma-Aldrich (St. Louis, MO, USA) if not stated otherwise. All chemicals were of analytical grade, and water was deionized (conductivity <0.1 μS/cm) or ultrapure Mili-Q laboratory grade. For all the measurements, we used nanobeads (Streptavidin Polystyrene Particles, 1% w/v, 0.7–0.9 μm, 10 mL Spherotech, Inc., Lake Forest, USA) modified with streptavidin and suspended in PBS (dilution 1:1000).

2.3. Dengue serum samples characterization with ELISA commercial kit

The Dengue serum (Code: DM1051) declared Positive for IgG immunoglobulins was obtained by Trina Bioreactives Ag. The serum was characterized in its content of IgG and IgM with the Dengue IgG ELISA kit (code: DENG.CE) manufactured by Dia.Pro Diagnostic BioProbes srl.

The test provides qualitative/semiquantitative determination of IgG antibodies to Dengue virus subtypes 1,2,3 and 4 in human plasma and serum. Microplates are coated with highly purified immunodominant recombinant Dengue virus antigens expressing all the 4 serotypes. In the first incubation (for 60 min at +37°), the solid phase is treated with diluted samples, and anti-Dengue virus IgG is captured, if present, by the antigens. After washing out all the other sample components, in the second incubation (for 60 min at +37°) bound anti-Dengue virus IgG are detected by adding anti hIgG antibody, labeled with peroxidase (HRP). The enzyme captured on the solid phase, acting on the substrate/chromogen mixture, generates an optical signal proportional to the amount of anti-Dengue virus IgG antibodies present in the sample.

For the following experiments, the positive Dengue IgG sample, characterized through ELISA, was diluted in two different matrices (PBS and Negative Human Serum for anti-Dengue IgG) with the following dilution sequence: PBS 1:100–1:12800 and negative human serum: 1:100–1:204800, in order to evaluate the DIS performance using real samples diluted with both a simple and complex matrix.

2.4. Microfluidic and electronic impedance measuring set-up

The microfluidic and the electronic measuring set-up are depicted in Fig. 1. The microfluidic system has been custom made in a transparent resin with stereolithography technique and consists of a microchamber (with a volume of 120 μL) with one inlet connected to a syringe pump and one outlet for waste. The microfluidic chamber and the chip surface are sealed together by an o-ring realized with a flexible elastomer, and the electrodes are contacted by pogo pins.

The electronic reading of the differential impedance of the biosensor chip has been performed by using a lock-in amplifier (HF2LI, Zurich Instruments AG, Switzerland). The sinusoidal voltage applied to one of the electrodes has been chosen with frequency in the range of 1 MHz to bypass the double layer capacitance but below the direct capacitance transfer in the liquid medium. The amplitude is 50 mV to avoid significant electrochemical reactions at the electrode surface. The currents from the IDE are detected by a transimpedance amplifier (TIA) (HF2TA, Zurich Instruments AG, Switzerland) with a gain of 10 kV/A and a bandwidth (3 dB cut-off) of 8 MHz. The lock-in bandwidth was set around 1Hz (time constant of 0.1 s) to allow a resolution better than 100 ppm, i.e., better than the desired resolution of the entire assay, ensuring sensor performance not to be limited by the measuring system.

The system allows implementing two DIS configurations: i) an analogic differential operation (see Fig. 1b) where two outputs of the HF2LI are used, one in counter phase to the other, and are applied to the external electrodes of the biosensor pair. The TIA is connected to the common central electrode and collects only the difference current generated by the unbalance of the pair upon bead deposition. ii) an offline digital differential operation (see Fig. 1c) where the output of the HF2LI is applied to both sensors of the pair, whose currents are independently collected by two TIAs and processed independently to perform the digital difference offline. All the reported measurements are done using this second configuration as it makes available the response of each sensor and allows to monitor every single step of the assay.

2.5. Protocol of the measurement

Experiments protocol (Fig. 2) consists of an "incubation phase" targeting specific primary antibody binding and labelling by secondary antibody, followed by a "beads counting phase" targeting nanobeads binding, impedance measurement and beads count. While this second phase is always performed in the microfluidic chamber, the incubation phase can also be conducted off-chamber.

In the LOD calculation experiments (incubation off-chamber) seven different chips spotted with peptide E01 were incubated with increasing concentrations of Rabbit anti-E01 IgG diluted in PBS (0 ng/mL, 0.1 ng/mL, 1 ng/mL, 10 ng/mL, 100 ng/mL, 1 μg/mL, 50 μg/mL). Chips were kept in a humid chamber for 2 h at room temperature, then they were rinsed with washing buffer (0.05M Tris HCl pH 9, 0.25 M NaCl, 0.05% Tween 20) for 10 min at room temperature and finally with PBS (10 min at room temperature). Chips were then incubated with biotinylated goat anti-rabbit IgG 1 μg/mL in a humid chamber for 1 h at room temperature. Chips were then washed as described in section 2.2. LOD was extrapolated from the impedance value of blank samples plus 3 standard deviations (3σ) using the linear range of the calibration curves (the equation used is: 3σ/s where s is the slope of calibration curve and σ is the standard deviation of impedance background in the control sample).

DENV incubations with human samples were entirely performed in the microfluidic chamber. In particular, the human samples containing antibodies against E01 are injected at a flow rate of 25 μL/min for 120 min with a continuous microinjection protocol for binding optimization. Next, the washing buffer is injected at a flow rate of 100 μL/min for the removal of possible the non-specific antibody binding. The secondary antibody (rabbit anti-human IgG; 1 μg/mL) is injected at the same flow rate and microinjection protocol for 60 min, followed by 15 min of washing buffer for impurity cleaning and a PBS injection to restore the initial conductivity of the liquid.

The beads counting step is common to both experiments. The beads suspension solution described in section 2.2 is injected at a flow rate of 50 μL/min for 30 min to guarantee beads sedimentation and streptavidinbiotin binding. Then the washing buffer solution is injected for about 10 min to remove the non-specific bindings, both on the active and on the reference sensor. Finally, a PBS solution is injected for few minutes to recover the conductivity level of the solution back to the starting value in order to detect the conductance variation only due to the presence of the beads bonded to the double antibody sandwich.

The impedance variation signals were plotted with a linear regression to calculate the limit of detection. LOD was extrapolated from the impedance value of blank samples plus 3 standard deviations (3σ). All the solutions injected in the microfluidic system were prepared in the same Tygon tubing and separated by microbubbles. The change of conductivity given by the microbubbles produces spikes in the recorded signal (see Fig. 3) that define the timing of the measurement. All assays are performed at room temperature.

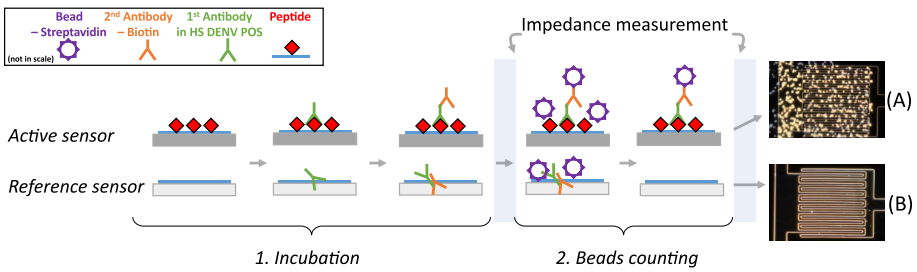

Fig. 2. Scheme of the protocol of the assay, subdivided into an Incubation phase followed by beads counting phase. On the far right, pictures of the biosensors after the final wash step: in (A) the active sensor with the bound polystyrene beads and in (B) the clean reference sensor.

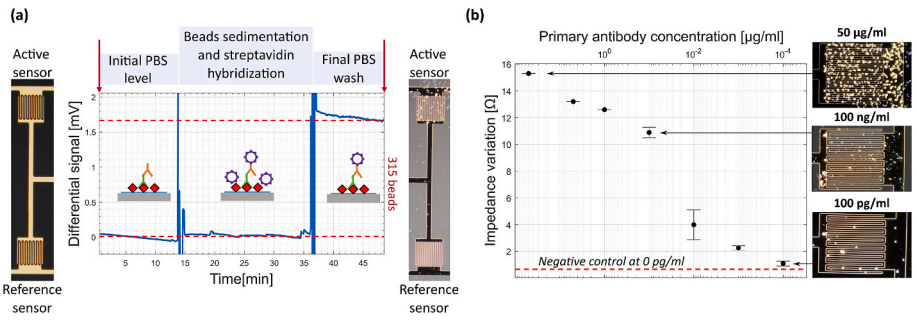

Fig. 3. (a) Time tracking of the measured Differential signal amplitude during the "beads counting phase" in the case of 10 ng/mL concentration of the anti-E01 IgG primary antibody. (b) DIS as a function of serial dilutions of anti-E01 IgG primary antibody at decreasing concentrations to assess the platform sensitivity in terms of LOD over a 10^6 concentration range. Error bars show standard error. The figures show the coverage of the active sensor by beads. All measurements have been performed with 50 mV amplitude signal at 1 MHz.

3. Results and discussion

3.1. Sensitivity and limit of detection of the platform for antibody detection

The biosensing system has been tested with serial dilutions of Rabbit anti-E01 IgG antibody at increasing concentrations (see section 2.5) to assess its sensitivity in terms of LOD. The chips were prepared off-chamber and were measured by performing the "beads counting phase" in the microfluidic chamber.

The graph in Fig. 3a reports the time evolution of the assay for the case of 10 ng/mL of the primary antibody. In the vertical axis there is directly the difference between the outputs of the two lock-in voltage signals of the active and the reference sensor. Minutes from 0 to 13 refer to injection of PBS and imbibition of both the active and reference sensors. This level of Differential signal will be the level to which all subsequent measurements will be referred to and is trimmed to zero according to the following equation.

$$A_{diff} = \left[\left(\frac{C_{act}}{C_{ref}}\right) \cdot X_{ref}\right] - X_{act}$$

where X_{act} and X_{ref} are the measured values proportional to the real part of the admittance for active and reference electrodes and C_{act} and C_{ref} are their average values calculated on the first 13 min. The small initial drift in Fig. 3a is due to the high salinity of the spotting agent used for the deposition of the peptide on the active sensor.

From 15 min to 35 min, the solution containing the streptavidin-coated beads is injected. Even though these beads hybridize only on the active sensor, where the secondary biotinylated antibody is present, they deposit everywhere on the chip surface due to the gravity force. Therefore, statistically, their deposition is not detectable in real-time in a Differential Impedance measurement, as demonstrated by the flatness of the level in this time interval. The beads selectively bound to the antibody become detectable during the last washing step. Thanks to the anti-fouling properties of the polymer coating, only the beads bound to an antibody against peptide E01 via biotin-streptavidin interaction remain on the sensor surface. Beads on the reference sensor, not selectively bounded, are washed away giving rise to an unbalance between the two sensors proportional to the actual unbalance of beads. The corresponding value compared to the initial condition gives the sought value correlated to the number of beads effectively hybridized on the active sensor. The picture on the right visualizes how effective is the bonding on the active sensor and how effective is the washing in cleaning the reference.

This experimental protocol has been repeated for different concentrations of primary antibody, from 50 μg/mL down to 100 pg/mL, to extract the LOD of the bioelectronic system. Fig. 3b summarizes these results. For antibody concentrations above 50 μg/mL, no significant change was observed due to the saturation of the binding sites with anti-IgG antibodies. On the other extreme, our DIS system demonstrates to operate down to a concentration of 100 pg/mL with signals (700 mΩ) well above the noise ground limit of 150 mΩ as present at the output of the lock-in amplifier. In particular, the LOD, calculated as reported in section 2.5, resulted to be 8.8 pg/mL. Negative controls using exactly the same protocol with zero concentration of primary antibody have given a mean value of 372 ± 90 mΩ, well below the signal measured at the minimum concentration of 100 pg/mL. Fig. 3b also shows the photographs of the active sensor surface taken at the end of the measurement after drying the chip. They clearly exhibit the corresponding decrease in beads density on the sensor's active area as the primary antibody concentration decreases. The platform tracks the number of beads that can be counted by impedance measurement down to few tens of beads, certifying the immunosensor concept and operation.

3.2. Anti-Dengue Virus antibodies detection with the DIS platform

In order to demonstrate the clinical effectiveness of the platform, our immunoassay-based biosensor system has been challenged to investigate the diagnosis of the viral disease of Dengue (DNGV) by detecting the antibodies present in the human sterilized serum of infected patients. In order to distinguish between the target and interference species that coexist in the blood and demonstrate the absence of false-positive signals, serum samples from healthy controls were tested as well. In these experiments, the complete assay has been performed in the microfluidic chamber, with both serum and beads incubation monitored in realtime through the Differential Impedance measurement.

Fig. 4a shows as an example the time evolution of the experiment in the case of a positive DNGV serum sample (dilution 1:10000) reporting the single independent signals available on each sensor (active and reference) and the differential one calibrated as discussed in section 3.1.

The initial level of impedance refers to the injection of PBS and imbibition of both active and reference sensors starting from different amplitude values. This level of Differential Impedance is trimmed to zero and will be the reference level which all subsequent measurements will be referred to. Then the serum solution containing the target antibody is injected at a very low rate for about 2 h. In this configuration, the first incubation selectively binds the primary antibody to the peptide on the sensing area. The unbalancing of the differential structure is undetectable due to the small size and low concentration of the primary antibody. After the washing step, the secondary antibody was injected for about 1 h. As in the previous step, there is no detectable unbalance between the two sensors. The final wash in washing buffer and PBS restores the surface conductivity for active and reference sensor. When the "beads counting phase" starts, streptavidin-coated beads were injected into the microfluidic chamber as described in section 3.1. The final value, obtained after the washing step provides the amplitude value that correlates with the number of beads effectively bound on the active sensor. This protocol has been applied to different dilutions of a serum sample positive to anti-Dengue antibody (characterized through ELISA as reported in section 2.3). Fig. 4b summarizes the DIS measurements at different dilutions of the serum sample positive to anti-Dengue antibody (from 1:25 to 1:100000). Healthy serum samples were included in the analysis as negative controls. Negative samples show a ground noise that we consider as a cut-off signal, with a DIS value

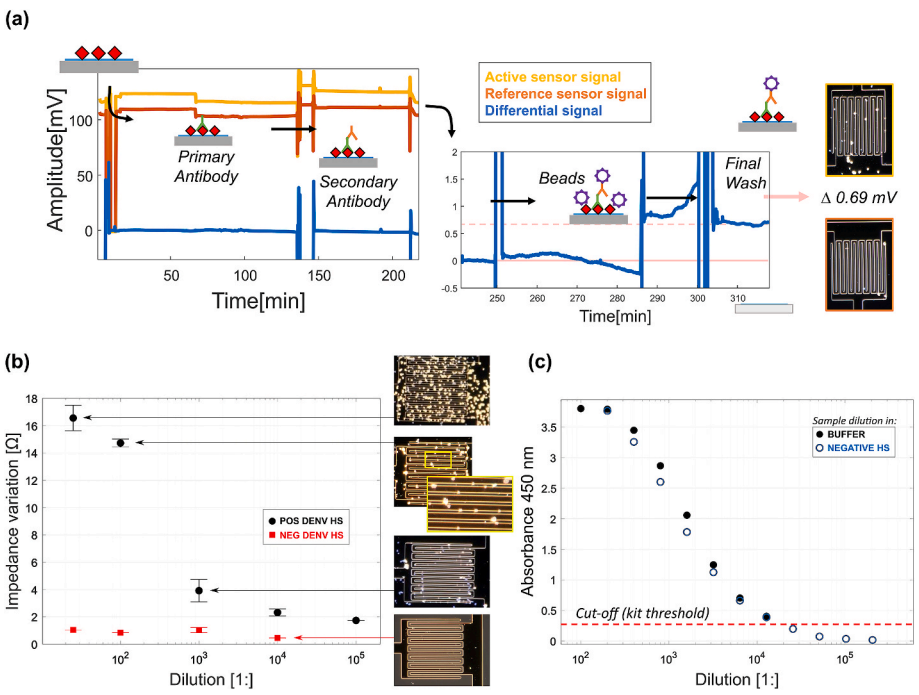

Fig. 4. (a) Time tracking of the signals during the incubation phase from the active sensor, the reference sensor and their differential signal. The differential signal, proportional to an unbalance of about 130 beads, is finally revealed upon washing with PBS. Photographs of the two electrodes after drying are shown on the right. (b), Differential Impedance sensing variation vs. dilution in a buffer of human serum positive to anti-Dengue Virus antibody. On the right, photographs of the active sensors after the final wash for four exemplary cases. Error bars show standard error. All measurements have been performed with 50 mV amplitude signal at 1 MHz. (c) Dengue virus IgG commercial kit results of absorbance at 450 nm vs. dilution in negative human serum or PBS buffer of the same positive Dengue virus serum sample used in our DIS biosensor.

below 1.23 Ω. As a consequence, the 1:100000 serum dilution provides the minimum detectable signal. The photographs of the active sensor surface visually certify the effectiveness of our detection mechanism for few exemplary dilutions and the number of beads over the active sensor decreases with sample dilution down to about one hundred. As can be seen in the magnification from Fig. 4b also clusters of beads are formed during washing and/or PBS evaporation contributing to the single concentrations error bar.

3.3. DIS platform and ELISA commercial kit on Anti-Dengue Virus antibodies detection

In order to certify the biosensor sensitivity and specificity, the same positive samples of human serum have been analyzed also with the kit "Enzyme Immunoassay (ELISA) for the qualitative/semi-quantitative determination of IgG antibodies to Dengue virus in human serum and plasma" (DIA.PRO, Diagnostic Bioprobes Srl, Milano, Italy). The ELISA experiment was performed according to the manufacturer's protocol (section 2.3) and the results are shown in Fig. 4c for samples diluted in two different matrices (Buffer and Negative Human Serum for anti-Dengue IgG). The higher number of dilutions in Fig. 4c was used to preliminary check the status of the serum sample and choose the correct range of concentrations to be tested with the DIS system. The Fig. 4c also shows the cut-off (threshold absorbance value) to discriminate the positives from the background as defined in the kit manufacturer's protocol. In conclusion, comparing the two figures Fig. 4b and c, the DIS method fully track the human serum positive to DENV certifying the validity of the method in early diagnosis of the disease down to 1:10^5 serum sample dilution.

4. Conclusions

Our work shows that beads count by a truly differential sensors architecture operated in a lock-in scheme is very effective in monitoring specific IgG antibodies in human serum and buffer down to few single counts resolution, i.e. a LOD of 88 pg/mL. The sensitivity obtained by the system reaches and possibly outperforms other methods yet operating in a simple and clear protocol as demonstrated in the comparison of the DIS platform response to human serum positive to DENV with a commercial Dengue virus IgG kit. The technique therefore has the potential to become a valuable early diagnostic tool when levels of circulating antibodies are still low and might go undetected by conventional methods, in particular in regions where sensitive ELISA and PCR methods are not readily available.

The system is perfectly suited to be easily configured for including novel probes able to detect concurrent viral strains or viral variants. Indeed, by simply modifying the preparation of the biosensor chip, the antibody and the probe, the Differential Impedance Sensing concept can address a wide range of pathogens and diseases, making it very flexible to approach industrial interest, yet reaching clinically breakthrough results in the initial stages of infection. The system is also ready to step into the realm of multivalent biosensors with multiple sensing sites operating in parallel on the same chip, allowing multiplex analysis from a single clinical sample by simply spotting different probes on different active sensors. Moreover, this proposed strategy paves the way for the development of lab-on-chip systems for the detection of infectious disease with increased sensitivity down to the single molecules detection.

Funding

This work was supported by Regione Lombardia, Grant numbers: 229472, title: READY – Network regionale per lo sviluppo di metodi diagnostici in risposta rapida a epidemie e bio emergenze.

CRediT authorship contribution statement

Paola Piedimonte: Experimental measurements and setup organization, Writing **Laura Sola:** Sample preparation and Writing Marina Cretich: Polymer synthesis **Alessandro Gori:** Biochemistry data analysis **Marcella Chiari:** Biochemistry Supervision **Edoardo Marchisio:** Sample human serum Dengue resources **Piero Borga:** State of art analysis **Riccardo Bertacco:** Funding and resources acquisition **Andrea Melloni:** Project administration **Giorgio Ferrari:** Electronic system Supervision **Marco Sampietro:** Writing and Project Coordinator.

Declaration of competing interest

The authors declare that they have no known competing financial

interests or personal relationships that could have appeared to influence the work reported in this paper.

Acknowledgments

The authors wish to thank the staff of Polifab, the nanofabrication facility of Politecnico, for the continuous support during the fabrication of the sensor chips and of the microfluidic chamber. Also, R. Ragusa for the help with the COMSOL simulations.

References

Alcon, S., Talarmin, A., Debruyne, M., Falconar, A., Deubel, V., Flamand, M., 2002. Enzyme-linked immunosorbent assay specific to dengue virus type 1 nonstructural protein NS1 reveals circulation of the antigen in the blood during the acute phase of disease in patients experiencing primary or secondary infections. J. Clin. Microbiol. 40 https://doi.org/10.1128/JCM.40.02.376-381.2002.

Austin Suthanthiraraj, P.P., Sen, A.K., 2019. Localized surface plasmon resonance (LSPR) biosensor based on thermally annealed silver nanostructures with on-chip blood-plasma separation for the detection of dengue non-structural protein NS1 antigen. Biosensors Bioelectron. 132 https://doi.org/10.1016/j.bios.2019.02.036.

Bergamaschi, G., Fassi, E.M., Romanato, A., D'Annessa, I., Odinolfi, M.T., Brambilla, D., Damin, F., Chiari, M., Gori, A., Colombo, G., Cretich, M., 2019. Computational analysis of dengue virus envelope protein (E) reveals an epitope with flavivirus immunodiagnostic potential in peptide microarrays. Int. J. Molecular Sci. 20 https://doi.org/10.3390/ijms20081921.

Berggren, C., Bjarnason, B., Johansson, G., 2001. Capacitive Biosensors. https://doi.org/10.1002/1521-4109(200103)13:3¡173::AIDELAN173¿3.0.CO;2-B.

Bertok, T., Lorencova, L., Chocholova, E., Jane, E., Vikartovska, A., Kasak, P., Tkac, J., 2019. Electrochemical Impedance Spectroscopy Based Biosensors: Mechanistic Principles, Analytical Examples and Challenges towards Commercialization for Assays of Protein Cancer Biomarkers. https://doi.org/10.1002/celc.201800848.

Bhatt, S., Gething, P.W., Brady, O.J., Messina, J.P., Farlow, A.W., Moyes, C.L., Drake, J. M., Brownstein, J.S., Hoen, A.G., Sankoh, O., Myers, M.F., George, D.B., Jaenisch, T., William Wint, G.R., Simmons, C.P., Scott, T.W., Farrar, J.J., Hay, S.I., 2013. The global distribution and burden of dengue. Nature 496. https://doi.org/10.1038/nature12060.

Carminati, M., Gervasoni, G., Sampietro, M., Ferrari, G., 2016. Note: differential configurations for the mitigation of slow fluctuations limiting the resolution of digital lock-in amplifiers. Rev. Sci. Instruments 87. https://doi.org/10.1063/1.4941721.

Carminati, M., Pedalà, L., Bianchi, E., Nason, F., Dubini, G., Cortelezzi, L., Ferrari, G., Sampietro, M., 2014. Capacitive detection of micrometric airborne particulate matter for solid-state personal air quality monitors. Sensors Actuators, A: Phy. 219 https://doi.org/10.1016/j.sna.2014.09.003.

Chowdhury, A.D., Takemura, K., Li, T.C., Suzuki, T., Park, E.Y., 2019. Electrical pulse-induced electrochemical biosensor for hepatitis E virus detection. Nat. Commun. 10 https://doi.org/10.1038/s41467-019-11644-5.

Cohen, L., Walt, D.R., 2019. Highly sensitive and multiplexed protein measurements. Chem. Rev. 119 https://doi.org/10.1021/acs.chemrev.8b00257.

Cretich, M., Bagnati, M., Damin, F., Sola, L., Chiari, M., 2011. Overcoming mass transport limitations to achieve femtomolar detection limits on silicon protein microarrays. Analytical Biochem. 418 https://doi.org/10.1016/j.ab.2011.07.004.

Darwish, N.T., Sekaran, S.D., Khor, S.M., 2018. Point-of-care Tests: A Review of Advances in the Emerging Diagnostic Tools for Dengue Virus Infection. https://doi.org/10.1016/j.snb.2017.09.159.

Desmet, C., Blum, L.J., Marquette, C.A., 2013. Multiplex microarray ELISA versus classical ELISA, a comparison study of pollutant sensing for environmental analysis. Environ. Sci.: Processes Impacts 15. https://doi.org/10.1039/c3em00296a.

Garrote, B.L., Santos, A., Bueno, P.R., 2019. Perspectives on and Precautions for the Uses of Electric Spectroscopic Methods in Label-free Biosensing Applications. https://doi.org/10.1021/acssensors.9b01177.

Gervasoni, G., Carminati, M., Ferrari, G., 2017. Switched ratiometric lock-in amplifier enabling sub-ppm measurements in a wide frequency range. Rev. Sci. Instruments 88. https://doi.org/10.1063/1.4996423.

Gori, A., Sola, L., Gagni, P., Bruni, G., Liprino, M., Peri, C., Colombo, G., Cretich, M., Chiari, M., 2016. Screening complex biological samples with peptide microarrays: the favorable impact of probe orientation via chemoselective immobilization strategies on clickable polymeric coatings. Bioconjugate Chem. 27 https://doi.org/10.1021/acs.bioconjchem.6b00426.

Guzman, M.G., Halstead, S.B., Artsob, H., Buchy, P., Farrar, J., Gubler, D.J., Hunsperger, E., Kroeger, A., Margolis, H.S., Martí-nez, E., Nathan, M.B., Pelegrino, J. L., Simmons, C., Yoksan, S., Peeling, R.W., 2010. Dengue: a continuing global threat. Nat. Rev. Microbiol. 8 https://doi.org/10.1038/nrmicro2460.

Herrada, C.A., Kabir, A., Altamirano, R., Asghar, W., 2018. Advances in diagnostic methods for Zika virus infection. J. Med. Dev. Transact. ASME 12. https://doi.org/10.1115/1.4041086.

Kabir, M.A., Ahmed, R., Iqbal, S.M.A., Chowdhury, R., Paulmurugan, R., Demirci, U., Asghar, W., 2021. Diagnosis for COVID-19: Current Status and Future Prospects. https://doi.org/10.1080/14737159.2021.1894930.

Lequin, R.M., 2005. Enzyme immunoassay (EIA)/enzyme-linked immunosorbent assay (ELISA). Clin. Chem. 51 https://doi.org/10.1373/clinchem.2005.051532.

Liang, T., Qu, Q., Chang, Y., Gopinath, S.C.B., Liu, X.T., 2019. Diagnosing ovarian cancer by identifying SCCantigen on a multiwalled carbon nanotube-modified dielectrode sensor. Biotechnol. Appl. Biochem. 66 https://doi.org/10.1002/bab.1808.

Lisdat, F., Schäfer, D., 2008. The Use of Electrochemical Impedance Spectroscopy for Biosensing. https://doi.org/10.1007/s00216-008-1970-7.

Martina, B.E., Koraka, P., Osterhaus, A.D., 2009. Dengue Virus Pathogenesis: an Integrated View. https://doi.org/10.1128/CMR.00035-09.

Merkoci, A., zhong Li, C., Lechuga, L.M., Ozcan, A., 2021. COVID-19 Biosensing Technologies. https://doi.org/10.1016/j.bios.2021.113046.

Messina, J.P., Brady, O.J., Golding, N., Kraemer, M.U., Wint, G.R., Ray, S.E., Pigott, D.M., Shearer, F.M., Johnson, K., Earl, L., Marczak, L.B., Shirude, S., Davis Weaver, N., Gilbert, M., Velayudhan, R., Jones, P., Jaenisch, T., Scott, T.W., Reiner, R.C., Hay, S. I., 2019. The current and future global distribution and population at risk of dengue. Nature Microbiology 4. https://doi.org/10.1038/s41564-019-0476-8.

Nadzirah, S., Azizah, N., Hashim, U., Gopinath, S.C., Kashif, M., 2015. Titanium dioxide nanoparticle-based interdigitated electrodes: a novel current to voltage DNA biosensor recognizes E. coli O157:H7. PLoS ONE 10. https://doi.org/10.1371/journal.pone.0139766.

Ohno, R., Ohnuki, H., Wang, H., Yokoyama, T., Endo, H., Tsuya, D., Izumi, M., 2013. Electrochemical impedance spectroscopy biosensor with interdigitated electrode for detection of human immunoglobulin A. Biosensors Bioelectron. 40 https://doi.org/10.1016/j.bios.2012.07.052.

Orazem, M.E., Tribollet, B., 2008. Electrochemical Impedance Spectroscopy. https://doi.org/10.1002/9780470381588.

Ozer, T., Geiss, B.J., Henry, C.S., 2020. Review—chemical and biological sensors for viral detection. Journal of The Electrochemical Society 167, 037523. https://doi.org/10.1149/2.0232003jes.

Pellitero, M.A., Shaver, A., Arroyo-Currás, N., 2020. Critical review—approaches for the electrochemical interrogation of DNA-based sensors: a critical review. J. Electrochem. Soc. 167 https://doi.org/10.1149/2.0292003jes.

Pinkova Gajdosova, V., Lorencova, L., Blsakova, A., Kasak, P., Bertok, T., Tkac, J., 2021. Challenges for Impedimetric Affinity Sensors Targeting Protein Detection. https://doi.org/10.1016/j.coelec.2021.100717.

Qureshi, A., Niazi, J.H., Kallempudi, S., Gurbuz, Y., 2010. Label-free capacitive biosensor for sensitive detection of multiple biomarkers using gold interdigitated capacitor arrays. Biosensors and Bioelectronics 25. https://doi.org/10.1016/j.bios.2010.03.018.

Singh, P., 2016. SPR Biosensors: Historical Perspectives and Current Challenges. https://doi.org/10.1016/j.snb.2016.01.118.

Sola, L., Damin, F., Gagni, P., Consonni, R., Chiari, M., 2016. Synthesis of clickable coating polymers by postpolymerization modification: applications in microarray technology. Langmuir 32 (40), 10284–10295. https://doi.org/10.1021/acs.langmuir.6b02816.

Strong, M.E., Richards, J.R., Torres, M., Beck, C.M., La Belle, J.T., 2021. Faradaic electrochemical impedance spectroscopy for enhanced analyte detection in diagnostics. Biosensors and Bioelectronics 177. https://doi.org/10.1016/j.bios.2020.112949.

Tancharoen, C., Sukjee, W., Thepparit, C., Jaimipuk, T., Auewarakul, P., Thitithanyanont, A., Sangma, C., 2019. Electrochemical biosensor based on surface imprinting for Zika virus detection in serum. ACS Sensors 4. https://doi.org/10.1021/acssensors.8b00885.

Wijaya, E., Lenaerts, C., Maricot, S., Hastanin, J., Habraken, S., Vilcot, J.P., Boukherroub, R., Szunerits, S., 2011. Surface Plasmon Resonance-Based Biosensors: from the Development of Different SPR Structures to Novel Surface Functionalization Strategies. https://doi.org/10.1016/j.cossms.2011.05.001.

Zhang, B., Salieb-Beugelaar, G.B., Nigo, M.M., Weidmann, M., Hunziker, P., 2015. Diagnosing Dengue Virus Infection: Rapid Tests and the Role of Micro/nanotechnologies. https://doi.org/10.1016/j.nano.2015.05.009.